Solar-Terrestrial Physics. 2022. Vol. 8. Iss. 4. P. 36–43. DOI: 10.12737/stp-84202203. © 2022 G.A. Makarov. Published by INFRA-M Academic Publishing House

UDC 550.385.4
DOI: 10.12737/stp-84202203

Received June 23, 2022
Accepted September 20, 2022

GEOMAGNETIC INDICES *ASY-H* AND *SYM-H* AND THEIR RELATION TO INTERPLANETARY PARAMETERS

G.A. Makarov
Yu.G. Shafer Institute of Cosmophysical Research and Aeronomy SB RAS, Yakutsk, Russia, gmakarov@ikfia.ysn.ru

Abstract. The dependences of the geomagnetic indices *SYM-H* and *ASY-H* on interplanetary parameters for the period from 1981 to 2015 according to their daily averages are studied. The study is carried out in two ways: the first — the entire data array is analyzed, the second — the data are divided into 9 activity groups in accordance with the average daily values of the planetary geomagnetic index A_p. A correlation analysis of the indices with the solar wind speed, magnitude, and the north-south component of the interplanetary magnetic field (IMF) has been performed. The search for a relationship between the *ASY-H* and *SYM-H* indices and interplanetary parameters turned out to be more successful when considering the entire data array than in the case of splitting the data into groups of magnetic activity. Regression equations relating *ASY-H* and *SYM-H* to interplanetary parameters are determined. It has been found that when describing the relationship between the *ASY-H* and *SYM-H* indices and the IMF north-south component, it is necessary to take into account the contribution of the IMF modulus.

Keywords: geomagnetic indices *SYM-H* and *ASY-H*, geomagnetic activity, magnetospheric ring current, interplanetary parameters, space weather.

INTRODUCTION

In the early years of direct spacecraft measurements of interplanetary plasma, a close relationship was found between geomagnetic activity and the solar wind velocity V [Snyder et al., 1963]. Then it was established that geomagnetic disturbances strongly depend on the interplanetary magnetic field (IMF): the modulus $|B|$, the southward component B_S [Wilcox et al., 1967], the azimuthal component B_y [Friis-Christensen et al., 1972], and IMF variability [Ballif et al., 1969].

As the amount of information on interplanetary parameters increased, such physical values as the interplanetary electric field [Rostoker, Falthammer, 1967], the electromagnetic energy flux from the solar wind [Akasofu, 1979], as well as various combinations of interplanetary medium parameters (coupling functions) began to be considered as geo-effective characteristics [Burton et al., 1975; Murayama et al., 1980; Holser, Slavin, 1982]. At an advanced level, the influence of solar wind parameters on geomagnetic activity is examined in detail in [Newell et al., 2007; Liemohn et al., 2018; Lockwood, McWilliams, 2021]. Newell et al. [2007] have compared ten variables characterizing magnetospheric conditions, including five geomagnetic indices and five characteristics of auroral and polar regions with more than twenty possible solar wind coupling functions; Liemohn et al. [2018] have analyzed the models predicting geomagnetic indices; Lockwood, McWilliams [2021] have studied the differences between optimal coupling functions for the transpolar voltage Φ_{PC}, the geomagnetic *am* index and the *SML* index of the auroral oval on the night side of the Northern Hemisphere. Note that the above works used observational data with minute or hour time resolution.

The state of the solar wind varies depending on solar conditions. The critical interplanetary parameter in the occurrence of magnetospheric disturbances is the IMF north-south component. Parameters of the solar wind vary greatly when high- and low-speed plasma flows and interplanetary magnetic clouds pass through it [Yermolaev et al., 2010]. Southward magnetic fields in high-speed solar wind streams and in corotating interaction regions can be the main source of energy for long-term geomagnetic activity on Earth [Echer et al., 2013]. Yermolaev et al. [2018] have shown that in such structures IMF $|B|$ and velocities of interplanetary currents are significantly increased. Most superstorms were caused by a shell preceding an interplanetary coronal mass ejection, or a combination of a shell and a magnetic cloud [Meng et al., 2019].

During geomagnetic storms, a ring current develops in the magnetosphere, whose intensity mainly determines the energy release there. When conducting research into solar-terrestrial relations and the space weather effect on the processes studied by related branches of science — meteorology, seismology, biophysics, in addition to planetary magnetic activity indices such as K_p, A_p, *aa*, etc., ring current indices, in our opinion, should be used. To estimate the magnetospheric ring current intensity, the low-latitude index *Dst* and the mid-latitude indices *SYM-H* and *ASY-H* have been developed. The *SYM-H* and *ASY-H* indices can identify the symmetric and asymmetric ring current components respectively [Iyemori et al., 1992]. Contributions of not only the ring current but also of magnetopause, magnetotail currents, and field-aligned currents to *Dst*, *SYM-H*, and *ASY-H* have been revealed to date [Alexeev et al., 1996; Maltsev et al., 1996; Tsyganenko, Sitnov, 2005]. The relationship between these

indices and the interplanetary parameters has been examined using one-minute data in [Weygand, McPherron, 2006; http://wdc.kugi.kyoto-u.ac.jp/aeasy/asy.pdf].

Solar-terrestrial relations are often studied by statistical methods with the use of daily average terrestrial, interplanetary, and solar parameters. It is well to bear in mind that with daily averaging of interplanetary parameters the indices of plasma and magnetic structures in the solar wind change and that with daily averaging of terrestrial parameters different phases of geomagnetic storms overlap each other; therefore, characteristics of storms (phases, intensity, duration, etc.) are leveled out. Nevertheless, it is interesting to analyze the relationship between daily average *SYM-H* and *ASY-H* indices on the one hand and the main interplanetary parameters on the other.

The purpose of this work is to investigate the dependence of the *SYM-H* and *ASY-H* indices on parameters such as the solar wind velocity *V*, the IMF modulus $|B|$ and normal, or north-south, component B_n through daily averaging of the data considered. In the future, it is planned to study the dependence of these indices on various solar wind coupling functions, derived from data on the main interplanetary parameters.

1. EXPERIMENTAL DATA IN USE

The work uses data on the geomagnetic indices *SYM-H* and *ASY-H* and the solar wind — its velocity *V*, the IMF modulus $|B|$ and normal component B_n for 1981–2015. The information on the indices has been taken from the archive of the World Data Center for Geomagnetism [https://wdc.kugi.kyoto-u.ac.jp/index.html]; and on the solar wind, from the website of the NASA Space Physics Data Center [http://omniweb.gsfc.nasa.gov]. The *SYM-H* and *ASY-H* indices have one-minute time resolution and are calculated from the geomagnetic field *H* component at six mid-latitude stations (the network includes more than ten stations). *SYM-H* is, in fact, an averaged deviation of *H* from the quiet level at the observation stations corrected for geomagnetic latitude, whereas *ASY-H* is defined as a range between maximum and minimum values of the *H* component after subtracting the corresponding symmetrical parts from the disturbance field. The method of determining these indices is described in detail in [Iyemori et al., 1992]. The IMF components have been used from the OMNI database in the RTN coordinate system: the R axis is directed radially from the Sun, the T axis is directed toward the solar rotation, and the N axis is the vector product of the R and T axes. At zero heliographic latitude, the N and solar rotation axes are parallel. The RTN and GSE coordinate systems at near-Earth distances differ in opposite directions of the R and X axes, as well as the T and Y axes respectively.

The days without data are excluded, so the number of days considered is 10759. The work is based on daily average data. Preliminary analysis of the relationship between the indices and the interplanetary parameters has shown that the closest correlation is obtained when comparing the indices with the key solar wind parameters — velocity, IMF modulus and north-south component (see Figure 1), whereas the relationship with dynamic pressure, electric field, and solar wind density is very weak: the correlation does not exceed 0.3, except for the relationship between *ASY-H* and the dynamic pressure with a correlation of 0.48.

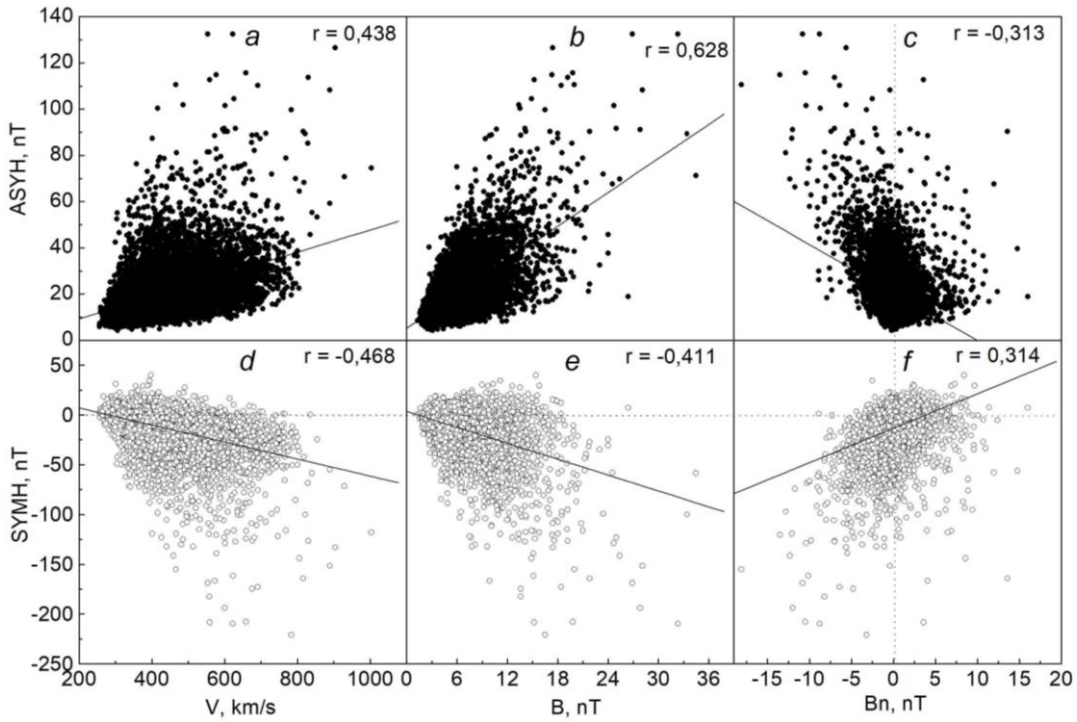

Figure 1. Distributions of daily average *ASY-H* and *SYM-H* as functions of coupling with the solar wind velocity *V* (*a*, *d*), the IMF modulus $|B|$ (*b*, *e*) and north-south component B_n (*c*, *f*) obtained across the dataset. In this and the following figures, *r* are linear correlation coefficients, solid lines are linear approximation of the corresponding data pairs, dotted lines are zero values of the corresponding parameter, the *SYM-H* index and the IMF B_n component in this case

Regression analysis of *SYM-H* and *ASY-H* on the one hand and V, $|B|$ and B_n on the other is carried out in two ways: the first — the entire data array is analyzed, the second — it is divided into activity groups, i.e. all data have been divided into nine groups in accordance with daily average A_p. Table 1 shows the number of days in the activity groups, average values, and standard deviations σ of the interplanetary parameters (V, $|B|$, B_n) and geomagnetic indices (A_p, *ASY-H*, *SYM-H*) in each activity group. It also gives information on the entire data array.

We can see (see Table 1) that with increasing geomagnetic activity, as expected from the data presented in the physical literature, the averages of interplanetary and geomagnetic parameters increase, with B_n gradually changing direction from north to south, and *SYM-H* increasing in modulus, standard deviations σ of the averages of interplanetary and geomagnetic data increasing with A_p; in the group $A_p \geq 27$, large σ for all the parameters are likely to result from a wide range of A_p variations.

2. RELATION OF THE *ASY-H* AND *SYM-H* INDICES TO INTERPLANETARY PARAMETERS

2.1. Results of analysis of the entire data array

Figure 1 illustrates distributions of the *ASY-H* and *SYM-H* indices as functions of coupling with the solar wind velocity V, the IMF modulus $|B|$ and north-south component B_n across the dataset. It follows from Figure 1 that the relationship exists and can be approximated by a linear equation of the type $y = ax + b$, where y is one of the indices; x is one of the interplanetary parameters; a is a regression coefficient; b is a free term. The regression coefficients a and the free terms b in the equations of the relationship between *ASY-H*, *SYM-H* and the interplanetary parameters V, $|B|$, and B_n are listed in Table 2 (see the row Entire dataset). This approach in describing the relation of the geomagnetic indices to the interplanetary parameters is applied for simplicity; note, however, that the magnetosphere responds to variations in solar wind conditions nonlinearly [Vaisberg et al., 2008].

Figure 1 shows that the relationship between both indices on the one hand and the solar wind velocity and the IMF modulus on the other is more pronounced. According to Table 2, we can say that *SYM-H* in absolute value depends on the solar wind velocity almost twice as much as *ASY-H*, and with respect to the IMF modulus both indices vary almost equally. The correlation of the indices with the IMF north-south component is less noticeable.

To figure this out, explore the relationship between the geomagnetic indices and the interplanetary parameters, dividing the entire data array into two subarrays depending on the sign of IMF B_n. Figure 2 shows the dependences of *ASY-H* and *SYM-H* on differently directed IMF B_n. In fact, Figure 2 presents the same as Figure 1, *c*, *f*, with the difference that the correlation analysis of the indices and B_n is carried out separately for $B_n > 0$ and $B_n \leq 0$. The correlation coefficients r in the linear approximation equations between *ASY-H* and B_n and *SYM-H* and B_n are 0.189 and –0.065 for $B_n > 0$ and –0.586 and 0.528 for $B_n \leq 0$ respectively. We can conclude that the ring current indices for northward IMF are almost independent of B_n, whereas for southward IMF both indices are noticeably related to B_n: with an increase in the absolute value of the IMF southward component B_S, the *ASY-H* and *SYM-H* indices increase in absolute value. The regression equations in this case can be written as *ASY-H*=–5.60 B_S+17.17 and *SYM-H*=8.09 B_S–8.53.

Table 1

Information on the intervals of A_p values, the number of days n, the average values and standard deviations σ of the geomagnetic indices *Ap*, *ASY-H*, *SYM-H* and the interplanetary parameters V, $|B|$, B_n in activity groups and across the dataset

A_p, nT	Number of days *n*	$<A_p>\pm\sigma$, nT	$<ASY\text{-}H>\pm\sigma$, nT	$<SYM\text{-}H>\pm\sigma$, nT	$<V>\pm\sigma$, km/s	$<B>\pm\sigma$, nT	$<B_n>\pm\sigma$, nT
0–2	841	1.60±0.63	10.90±2.85	–2.08±5.96	338.17±44.02	3.71±1.35	0.33±0.89
3–5	2609	4.02±0.75	13.92±3.81	–4.29±8.01	375.30±54.20	4.72±1.52	0.30±1.14
6–8	2219	6.88±0.84	17.00±4.39	–8.02±10.18	416.34±67.92	5.75±1.74	0.14±1.29
9–11	1357	9.94±0.78	19.80±4.89	–11.38±11.72	447.70±77.91	6.42±1.95	0.07±1.50
12–14	950	12.90±0.86	21.91±5.20	–14.24±12.32	472.86±87.79	6.99±2.15	0.02±1.49
15–17	624	15.98±0.78	24.32±5.76	–17.40±13.41	485.81±93.24	7.32±2.32	–0.16±1.73
18–20	511	18.95±0.84	26.90±6.30	–21.21±14.62	509.06±98.32	7.75±2.46	–0.20±1.78
21–26	630	23.34±1.78	29.71±7.07	–24.34±14.91	528.37±99.66	8.31±2.76	–0.28±1.91
≥27	1018	44.80±23.79	43.22±15.95	–45.15±30.70	553.23±113.02	10.40±3.98	–1.01±3.06
Entire dataset	10759	12.34±14.02	20.68±11.02	–13.26±18.33	437.17±100.32	6.31±2.83	0.01±1.66

Table 2

Regression coefficients *a* and free terms *b* in linear approximation equations between the geomagnetic indices *ASY-H*, *SYM-H* and the interplanetary parameters *V*, |*B*|, B_n obtained across the dataset and at different signs of IMF B_n

IMF B_n sign	Number of days	Index	*V*		|*B*|		B_n	
			a	*b*	*a*	*b*	*a*	*b*
Entire dataset	10759	*ASY-H*	0.05	–0.33	2.45	5.23	–2.08	20.70
		SYM-H	–0.09	24.12	–2.66	3.54	3.46	–13.29
$B_n>0$	5089	*ASY-H*	0.04	–0.90	1.79	7.32	1.23	17.44
		SYM-H	–0.08	26.42	–1.50	–0.48	–0.76	–9.26
$B_n\leq0$	5670	*ASY-H*	0.05	0.21	3.11	3.01	–5.60	17.17
		SYM-H	–0.09	22.02	–3.82	7.72	8.09	–8.53

From the data presented in Table 2 we can conclude that *a* and *b* in the equations of relationship of *ASY-H* and *SYM-H* with *V* and |*B*| across the dataset represent the averages of the results of their summing at $B_n>0$ and $B_n\leq0$. Note that the dependences of the *ASY-H* and *SYM-H* indices on the solar wind velocity at differently directed IMF B_n do not change. It has to be said that the correlation coefficients between *V* and B_n for both signs of B_n are lower than 0.018, which indicates that *V* and IMF B_n are independed of each other. *V* and |*B*| ($r<0.22$) are almost independent of each other. This information has been obtained by comparing the parameters separately. The nature of the dependence of *ASY-H* and *SYM-H* on the IMF modulus is not the same for different IMF B_n signs — for southward IMF the correlation coefficients between *ASY-H* and *SYM-H* on the one hand and |*B*| on the other are noticeably higher than for northward IMF: for *ASY-H* r=0.70 and r=0.58 respectively; for *SYM-H* r=–0.54 and r=–0.27 respectively. Thus, the relationship between the indices and the IMF modulus when taking into account the IMF B_n sign is similar to the relationship between the indices and IMF B_n in Figure 2.

Figure 3 shows the ratios between |*B*| and B_n for southward and northward IMF, obtained across the dataset.

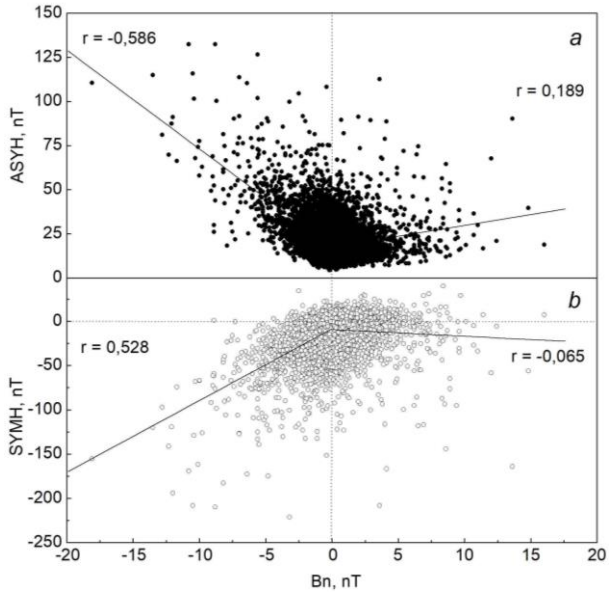

Figure 2. Distributions of daily average *ASY-H* (*a*) and *SYM-H* (*b*) as functions of coupling with the IMF north-south component B_n, obtained across the dataset, taking into account the B_n sign: for southward IMF (left), for northward IMF (right)

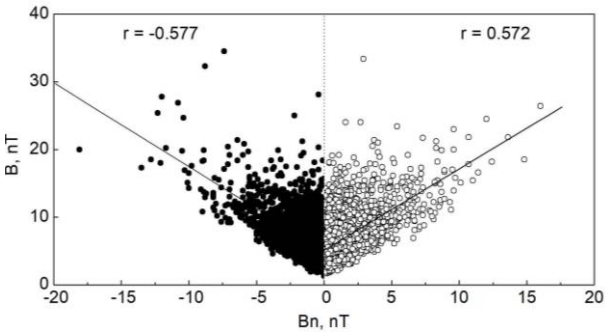

Figure 3. Ratios between |*B*| and B_n for southward (left) and northward (right) IMF, obtained across the dataset

The regression equations are as follows: for southward IMF $|B|=-1.24\ B_S+5.07$, for northward IMF $|B|=1.20\ B_N+5.12$. The dependences are seen to be the same — the coefficients *a* and the free terms *b* are almost equal, takinginto account the B_n sign. Nonetheless, the *ASY-H* and *SYM-H* indices exhibit different dependence on |*B*| and B_n for different IMF directions (see Figure 2, Table 2). It is obvious that such a picture results from the response of intramagnetospheric processes to IMF direction. It is known [Lockwood, McWilliams, 2021] that the mechanisms of penetration of energy from the solar wind into the magnetosphere at southward and northward IMF differ. And the fact that the correlation coefficients between *ASY-H* and IMF |*B*| in both directions of B_n are higher than those between *SYM-H* and IMF |*B*| probably reflects the nature of these indices — *SYM-H* characterizes the intensities of the symmetric component of the magnetospheric ring current and magnetopause and tail currents; and *ASY-H* describes the intensity of the asymmetric ring current component and the current systems containing magnetospheric-ionospheric field-aligned currents [Dubyagin et al., 2014].

Estimate the contributions of IMF |*B*| to *ASY-H* and *SYM-H* and subtract them from experimental values of the indices. To do this, we use the regression coefficients *a* and the free terms *b* in the linear approximation equations between *ASY-H*, *SYM-H* and IMF |*B*| from Table 2. Figure 4 depicts the differences obtained after excluding the calculated contributions of *ASY-H*(|*B*|) and *SYM-H*(|*B*|) from experimental values of the indices. Distributions of the differences between *ASY-H*–*ASY-H*(|*B*|) and *SYM-H*–*SYM-H*(|*B*|) relative to the IMF north-south component without separating by the B_n sign are presented in panels *a* and *d*; for $B_n\leq0$, in panels

b and *e*; for $B_n>0$, in panels *c* and *f* respectively. The data is seen to be distributed quite naturally — with decreasing IMF northward component and increasing IMF southward component, the differences increase from negative values to positive ones for *ASY-H–ASY-H*(|*B*|) and vice versa for *SYM-H–SYM-H*(|*B*|). Recall that panels *b* and *e* present the differences between the indices for southward IMF; panels *c* and *f*, for the northward one. We have to admit that this method of searching for the relationship of the indices with the B_n component is ineffective since the correlation of the data compared in panels *b*, *c*, *e*, *f* is low. Preference should therefore be given to considering the relationship of the indices with B_n when the data array is not divided according to the B_n sign (panels *a* and *d*), but taking into account the contribution of IMF |*B*|. The correlation coefficient between *ASY-H–ASY-H*(|*B*|) and B_n is higher than 0.4, and between *SYM-H–SYM-H*(|*B*|) and B_n is higher than 0.5. We can conclude that after excluding the contribution of the IMF modulus, the *ASY-H* and *SYM-H* indices show a linear correlation with the IMF north-south component: their absolute values increase as B_n turns from north to south, with *SYM-H* increasing almost three times more than *ASY-H*. The corresponding regression equations can be written as follows: $\Delta ASY\text{-}H=ASY\text{-}H–ASY\text{-}H(|B|)=–2.11\ B_n+0.07$ and $\Delta SYM\text{-}H=SYM\text{-}H–SYM\text{-}H(|B|)=6.12B_n–16.91$.

Examine the behavior of *ASY-H* and *SYM-H* when daily average B_n is zero. During the period of interest there were 118 such days. Figure 5 shows distributions of the *ASY-H* and *SYM-H* indices relative to the solar wind velocity (*a*) and the IMF modulus (*b*). Figure 5 indicates that the dependences of *ASY-H* on *V* and of *SYM-H* on |*B*| do not manifest themselves, but there is a moderate correlation in the relations *ASY-H* — |*B*| and *SYM-H* — *V*: with increasing |*B*|, *ASY-H* increases; with increasing *V*, *SYM-H* increases. The *SYM-H* index characterizes the symmetric component of the ever-present ring current and the tail and magnetopause currents, whereas the *ASY-H* index reflects their asymmetric component that occurs during magnetospheric disturbances [Iyemori et al., 1992]. In this case, in the absence of IMF B_n, with increasing *V* the magnetosphere experiences compression such that the ring current and the magnetopause and magnetotail current systems intensify, and with increasing |*B*| the transfer of the interplanetary electric field into the magnetosphere increases which causes current systems to enhance and a partial ring current to appear. In this sample, the average of $<ASY\text{-}H>=(10.8\pm2.9)$ nT, and $<SYM\text{-}H>=(–2.2\pm5.5)$ nT; these values are close to the offsets of *ASY-H* and *SYM-H* determined when studying the dependence of these indices on the level of magnetic activity [Makarov, 2021].

2.2. Results of the analysis of averages in groups of magnetic activity

Examine the relationship of the *ASY-H* and *SYM-H* indices with interplanetary parameters from their averages in the groups of magnetic activity. Table 1 lists averages of *ASY-H* and *SYM-H*, *V*, |*B*|, and B_n in the groups

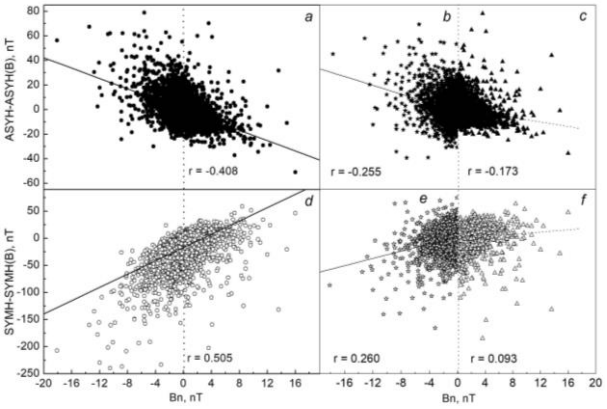

Figure 4. Distributions of daily average differences between *ASY-H–ASY-H*(|*B*|) (*a–c*) and *SYM-H–SYM-H*(|*B*|) (*d–f*) as functions of coupling with the IMF north-south component B_n obtained across the dataset without separation (*a*, *d*) and with separation (*b*, *c*, *e*, *f*) according to B_n sign

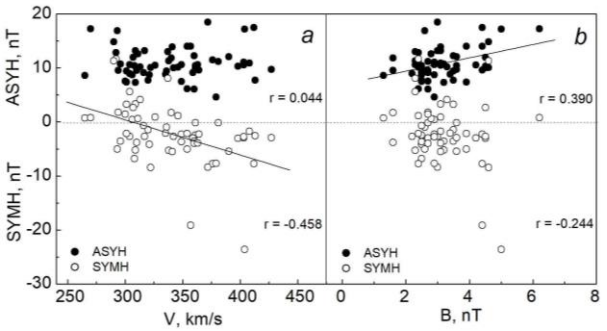

Figure 5. Distributions of daily average *ASY-H* and *SYM-H* relative to the solar wind velocity *V* (*a*) and the IMF modulus |*B*| (*b*) at $B_n=0$

of magnetic activity. The correlation coefficients *r* calculated for each pair of the values compared show that the relationships between the indices and the interplanetary parameters are almost functional: for *ASY-H* $r>0.97$, for *SYM-H* $r>0.94$. This can be explained by a small number of groups of magnetic activity and by operating with the data averaged in the groups. The increase in the indices with increasing *V*, |*B*| and decreasing B_n is clearly visible, i.e. with the change in the IMF direction from north to south.

Examine the relationship between *ASY-H*, *SYM-H* and B_n by dividing the data into two parts according to B_n sign, as in the previous section. Figure 6 shows dependences of *ASY-H* and *SYM-H* on B_n, obtained separately at $B_n\le0$ and $B_n>0$; the corresponding regression characteristics are given in Table 3. We can see that, unlike the similar picture across the dataset (Figure 2), in Figure 6 at southward and northward IMF with an increase in the absolute value of B_n the *ASY-H* and *SYM-H* indices also increase in absolute value. It turns out that at northward IMF with increasing B_n magnetic activity increases. To clarify such an unexpected result, as above, examine the relationship between |*B*| and B_n at $B_n>0$ and $B_n\le0$ for the average values in the groups of magnetic activity.

Figure 7 shows the correlations between |*B*| and B_n for southward (left) and northward (right) IMF. As for the entire dataset (see Figure 3), |*B*| increases proportionally

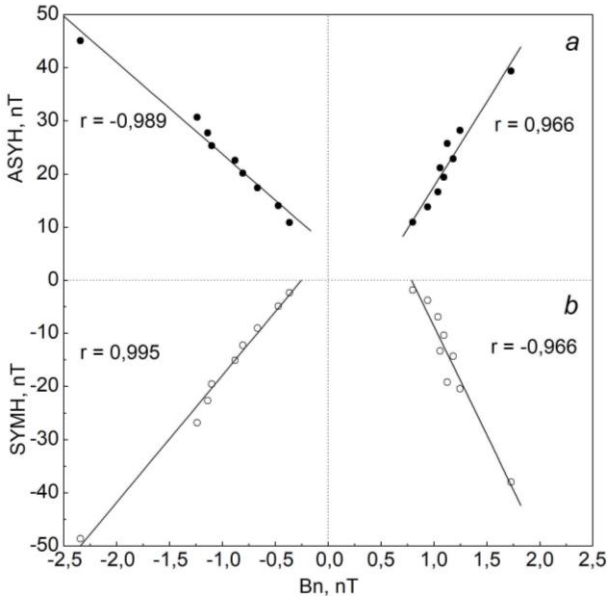

Figure 6. Distributions of *ASY-H* (*a*) and *SYM-H* (*b*) as functions of coupling with the IMF north-south component B_n by their averages in the groups of magnetic activity with the B_n sign taken into account: for southward (left) and northward (right) IMF

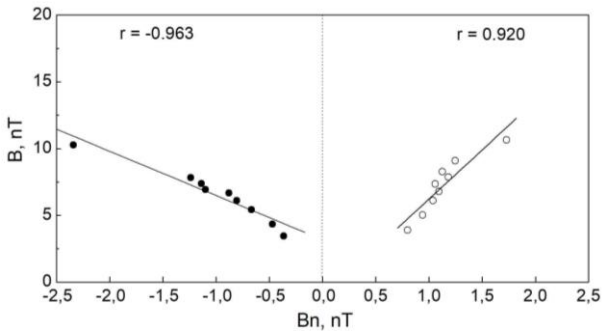

Figure 7. Ratio between $|B|$ and B_n at southward (left) and northward (right) IMF according to their averages in the groups of magnetic activity

with the increase in the absolute value of B_n at $B_n>0$ and $B_n\leq 0$. The linear regression equations for southward and northward IMF take the form $|B|=-3.31\ B_S+3.18$ and $|B|=7.35\ B_N-1.12$ respectively. The regression coefficients *a* in these equations are seen to differ markedly from those for the entire data array.

Estimate the contributions of the IMF modulus to *ASY-H* and *SYM-H* and subtract them from the experimental values of the indices. For this purpose, apply the regression coefficients *a* and the free terms *b* in the linear approximation equations between the geomagnetic indices *ASY-H*, *SYM-H* and the IMF modulus $|B|$ separately for $B_n\leq 0$ and $B_n>0$ from Table 3. The differences obtained after excluding the calculated contributions of *ASY-H*(*B*) and *SYM-H*(*B*) from the experimental values of the indices and by taking into account the sign of the IMF north-south component $B_n\leq 0$ and $B_n>0$ are distributed randomly, without a certain regularity. In these relations and also if the B_n sign is ignored, the correlation between the differences *ASY-H*–*ASY-H*($|B|$) and *SYM-H*–*SYM-H*($|B|$) on the one hand and B_n on the other does not exceed 0.3. It follows that the IMF modulus contribution levels the dependence of *ASY-H* and *SYM-H* on B_n when considering this dependence separately for southward and northward IMF. Thus, the study into the relationship of *ASY-H* and *SYM-H* with B_n by dividing data into groups according to the level of magnetic activity can be carried out without grouping the data by the B_n sign.

2.3. Comparison of relationships obtained from different data samples

If we compare the information presented in Tables 2, 3 (rows Entire dataset), we can notice some differences. For example, the regression coefficients *a* in the case of the relationship of the indices with the solar wind velocity *V* and the IMF modulus $|B|$ are quite close for different samples, but in the case of the relationship with the IMF north-south component B_n the coefficients *a* differ greatly — almost by an order of magnitude. It is fair to assume that this depends on data sampling. For the entire array of daily average data, the range of variations in *ASY-H* is approximately 140 nT; in *SYM-H*, ~275 nT; in *V*, ~800 km/s, in *B*, ~35 nT; in B_n,~35 nT. If we operate with data averaged over the groups of magnetic activity, the following values are observed: *ASY-H*~35 nT, *SYM-H*~45 nT, *V*~250 km/s, *B*~7 nT, B_n~1.5 nT. The ratios between the ranges of the corresponding data across the entire dataset and activity groups are ~4 for *ASY-H*, ~6 for *SYM-H*, ~3 for *V*, ~5 for $|B|$, ~24 for B_n; i.e only for B_n an abnormally large ratio is obtained which probably determines the strong difference in the coefficients *a* in Tables 2, 3. When we analyze the relationship between the indices and B_n in the activity

Table 3

Regression coefficients *a* and free terms *b* in linear approximation equations between the *ASY-H*, *SYM-H* indices, averaged over the groups of magnetic activity, and the interplanetary parameters *V*, $|B|$, B_n regardless of the B_n sign and at different B_n signs

IMF B_n sign	Index	*V*		$\|B\|$		B_n	
		a	*b*	*a*	*b*	*a*	*b*
Entire dataset	*ASY-H*	0.10	–21.97	3.92	–4.36	–27.42	21.02
	SYM-H	–0.12	38.45	–4.76	17.07	33.67	–13.63
$B_n>0$	*ASY-H*	0.11	–28.00	4.04	–7.16	31.90	–14.20
	SYM-H	–0.13	47.89	–5.05	22.28	–41.01	32.32
$B_n\leq 0$	*ASY-H*	0.13	–36.48	5.02	–8.86	–17.32	6.43
	SYM-H	–0.18	61.97	–6.79	26.17	23.92	6.00

groups, we average the data in them and thereby reduce the range of their values. As for the free terms *b*, they are determined by the spread of data in the samples (see Table 1).

When dealing with the entire array of daily average data, the *SYM-H* index in absolute value depends on the solar wind velocity almost twice as much as the *ASY-H* index, and relative to the IMF modulus both indices vary almost equally. The correlation of the indices with the IMF north-south component is less pronounced (see Figure 1). Given that IMF $|B|$ and B_n vary proportionally, to identify the dependence of the *ASY-H* and *SYM-H* indices on B_n account must be taken of their relationship with $|B|$.

When operating with data averaged over the groups of magnetic activity, the increases in the absolute values of the indices with an increase in *V*, $|B|$ are more uniform, and their increase with a decrease in B_n is also obvious, i.e. with the change in the IMF direction from north to south (see Table 1).

CONCLUSION

The statistical relationship of the magnetospheric ring current geomagnetic indices *ASY-H* and *SYM-H* with the main interplanetary parameters (the solar wind velocity *V*, the IMF modulus $|B|$ and normal (north-south) component B_n) has been studied. The daily average values for 1981–2015 were used. Regression analysis of the data in the linear approximation assumption was carried out in the first case for the entire data array, in the second for the average data divided into groups according to the daily average values of the planetary geomagnetic index A_p.

The following results have been obtained:

1. It has been shown that it is preferable to determine the relationship of the magnetospheric ring current geomagnetic indices *ASY-H* and *SYM-H* with the main interplanetary parameters by considering the entire data array rather than by dividing the data into groups of magnetic activity.

2. Regression equations describing the dependences of the daily average values of *ASY-H* and *SYM-H* on the solar wind velocity, the IMF modulus $|B|$ and north-south component B_n have been defined.

3. It has been found that when describing the relationship of the magnetospheric ring current geomagnetic indices *ASY-H* and *SYM-H* with the IMF north-south component B_n, consideration must be given to the contribution of the IMF modulus $|B|$.

The results of the work can be used to study the large-scale patterns of the interaction between the solar wind and Earth's magnetosphere such as seasonal and cyclic variations in geomagnetic activity, and can also be useful in examining solar-terrestrial relations and manifestations of space weather in processes investigated in meteorology, seismology, biophysics, etc.

The work was carried out under Government assignment (State Registration Number 122011700182-1).

REFERENCES

Akasofu S.-I. Interplanetary energy flux associated with magnetospheric substroms. *Planet. Space Sci*. 1979, vol. 27, iss. 4, pp. 425–431. DOI: 10.1016/0032-0633(79)90119-3.

Alexeev I.I., Belenkaya E.S., Kalegaev V.V., Feldstein Y.I., Grafe A. Magnetic storms and magnetotail currents. *J. Geophys. Res*. 1996, vol. 101, iss. A4, pp. 7737–7747. DOI: 10.1029/95JA03509.

Ballif J.R., Jones D.E., Coleman P.J. Further evidence on the correlation between transverse fluctuations in the interplanetary magnetic field and K_p. *J. Geophys. Res.* 1969, vol. 74, iss. 9, pp. 2289–2301. DOI: 10.1029/JA074i009p02289.

Burton R.K., McPherron R.L., Russell C.T. An empirical relationship between interplanetary conditions and *Dst*. *J. Geophys. Res*. 1975, vol. 80, iss. 31, pp. 4204–4214. DOI: 10.1029/ja080i031p04204.

Dubyagin S., Ganushkina N., Kubyshkina M., Liemohn M. Contribution from different current systems to *SYM* and *ASY* midlatitude indices. *J. Geophys. Res*. 2014, vol. 119, pp. 7243–7263. DOI: 10.1002/2014JA020122.

Echer E., Tsurutani B.T., Gonzalez W.D. Interplanetary origins of moderate (–100 nT < *Dst* ≤ –50 nT) geomagnetic storms during solar cycle 23 (1996–2008). *J. Geophys. Res.* 2013, vol. 118, iss. 1, pp. 385–392. DOI: 10.1029/2012JA018086.

Friis-Christensen E., Lassen K., Wilhjelm J., Wilcox J.M., Gonzalez W., Colburn D.S. Critical component of the interplanetary magnetic field responsible for large geomagnetic effects in the polar cap. *J. Geophys. Res.* 1972, vol. 77, iss 19, pp. 3371–3376. DOI: 10.1029/JA077i019p03371.

Holser R.E., Slavin J.A. An evaluation of three predictors of geomagnetic activity. *J. Geophys. Res.* 1982, vol. 87, iss. A4, pp. 2558–2562. DOI: 10.1029/JA087iA04p02558.

Iyemori T., Araki T., Kamei T., Takeda M. *Mid-latitude geomagnetic indices ASY and SYM (Provisional) No. 1 (1989–1990).* Data Analysis Center for Geomagnetism and Space Magnetism; Kyoto University, Kyoto, 1992, 110 p.

Liemohn M.W., McCollough J.P., Jordanova V.K., Ngwira C.M., Morley S.K., Cid C., et al. Model evaluation guidelines for geomagnetic index predictions. *Space Weather*. 2018, vol. 16, pp. 2079–2102. DOI: 10.1029/2018SW002067.

Lockwood M., McWilliams K.A. On optimum solar wind magnetosphere coupling functions for transpolar voltage and planetary geomagnetic activity. *J. Geophys. Res*. 2021, vol. 126, e2021JA029946. DOI: 10.1029/2021JA029946.

Makarov G.A. Offset in the geomagnetic indices of the magnetospheric ring current. *Solar-Terr. Phys.* 2021, vol. 7, iss. 3, pp. 29–35. DOI: 10.12737/stp-73202103.

Maltsev Y.P., Arykov A.A., Belova E.G., Gvozdevsky B.B., Safargaleev V.V. Magnetic flux redistribution in the storm time magnetosphere. *J. Geophys. Res.* 1996, vol. 101, no. A4, pp. 7697–7704. DOI: 10.1029/95JA03709.

Meng X., Tsurutani B.T., Mannucci A.J. The solar and interplanetary causes of superstorms (minimum *Dst*≤–250 nT) during the space age. *J. Geophys. Res.* 2019, vol. 124, iss. 6, pp. 3926–3948. DOI: 10.1029/2018JA026425.

Murayama T., Aoki T., Nakai H., Hakamada K. Empirical formula to relate the auroral electrojet intensity with interplanetary parameters. *Planet. Space Sci.* 1980, vol. 28, iss. 8, pp. 803–813. DOI: 10.1016/0032-0633(80)90078-1.

Newell P.T., Sotirelis T., Liou K., Meng C.-I., Rich F.J. A nearly universal solar wind-magnetosphere coupling function inferred from 10 magnetospheric state variables. *J. Geophys. Res.* 2007, vol. 112, A01206. DOI: 10.1029/2006JA012015.

Rostoker G., Falthammer C.-G. Relationship between changes in the interplanetary magnetic field and variations in

the magnetic field at the Earth's surface. *J. Geophys. Res.* 1967, vol. 72, iss. 23, pp. 5853–5863. DOI: 10.1029/JZ072i023p05853.

Snyder C.W., Neugebauer M., Rao N.R. The solar wind velocity and its correlation with cosmic ray variations and with solar and geomagnetic activity. *J. Geophys. Res.* 1963, vol. 68, iss. 24, pp. 6361–6370. DOI: 10.1029/JZ068i024p06361.

Tsyganenko N.A., Sitnov M.I. Modeling the dynamics of the inner magnetosphere during strong geomagnetic storms. *J. Geophys. Res.* 2005, vol. 110, A03208. DOI: 10.1029/2004JA010798.

Vaisberg O.L., Smirnov V.N., Zastenker G.N., Savin S.P., Verigin M.I. *Plazmennaya geliogeofizika. T. 1: Vzaimodeistvie solnechnogo vetra s vneshnei magnitosferoi Zemli* [Plasma Geliogeophysics. Ed. L.M. Zeleny, I.S. Veselovsky. Vol. 1: Interaction of the solar wind with the outer magnetosphere of the Earth]. Moscow, FIZMATLIT Publ., 2008. P. 378–422. (In Russian).

Weygand J.M., McPherron R.L. Dependence of ring current asymmetry on storm phase. *J. Geophys. Res.* 2006, vol. 111, A11221. DOI: 10.1029/2006JA011808.

Wilcox J.M., Schatten K.H., Ness N.F. Influence of interplanetary magnetic field and plasma on geomagnetic activity during quiet-sun condition. *J. Geophys. Res.* 1967, vol. 72, iss. 1, pp. 19–26. DOI: 10.1029/JZ072i001p00019.

Yermolaev Yu.I., Lodkina I.G., Nikolaeva N.S., Yermolaev M.Yu. Statistical study of interplanetary condition effect on geomagnetic storms. *Cosmic Research*. 2010, vol. 48, iss. 6, pp. 485–500. DOI: 10.1134/S0010952510060018.

Yermolaev Yu.I., Lodkina I.G., Nikolaeva N.S., Yermolaev M.Yu., Riazantseva M.O., Rakhmanova L.S. Statistic study of the geoeffectiveness of compression regions CIRs and Sheaths. *J. Atmos. Solar-Terr. Phys*. 2018, vol. 180, pp. 52–59. DOI: 10.1016/j.jastp.2018.01.027.

URL: http://wdc.kugi.kyoto-u.ac.jp/aeasy/asy.pdf (accessed March 29, 2022).

URL: http://omniweb.gsfc.nasa.gov (accessed March 29, 2022).

URL: https://wdc.kugi.kyoto-u.ac.jp/index.html (accessed March 29, 2022).

Original Russian version: Makarov G.A., published in Solnechno-zemnaya fizika. 2022. Vol. 8. Iss. 4. P. 38–45. DOI: 10.12737/szf-84202203.

How to cite this article

Makarov G.A. Geomagnetic indices ASY-H and SYM-H and their relation to interplanetary parameters. *Solar-Terrestrial Physics*. 2022. Vol. 8. Iss. 4. P. 36–43. DOI: 10.12737/stp-84202203.